

# Shallow Decay of Early X-ray Afterglows from Inhomogeneous Gamma-Ray Burst Jets

Kenji Toma<sup>1</sup>, Kunihito Ioka<sup>1</sup>, Ryo Yamazaki<sup>2</sup>, and Takashi Nakamura<sup>1</sup>

## ABSTRACT

Almost all the X-ray afterglows of gamma-ray bursts (GRBs) observed by the *Swift* satellite have a shallow decay phase in the first thousands of seconds. We show that in an inhomogeneous jet (multiple-subjet or patchy-shell) model the superposition of the afterglows of off-axis subjets (patchy shells) can have the shallow decay phase. The necessary condition for obtaining the shallow decay phase is that  $\gamma$ -ray bright subjets (patchy shells) should have  $\gamma$ -ray efficiency higher than previously estimated, and should be surrounded by  $\gamma$ -ray dim subjets (patchy shells) with low  $\gamma$ -ray efficiency. Our model predicts that events with dim prompt emission have the conventional afterglow light curve without the shallow decay phase like GRB 050416A.

*Subject headings:* gamma rays: bursts — gamma rays: theory

## 1. Introduction

Before the *Swift* era, most of the X-ray and optical afterglows of gamma-ray bursts (GRBs) were detected only several hours after the burst trigger. *Swift* observations are unveiling the first several hours of the afterglows (e.g., Tagliaferri et al. 2005; Chincarini et al. 2005; Nousek et al. 2005; Cusumano et al. 2005; Hill et al. 2005; Vaughan et al. 2005). Recently, Nousek et al. (2005) analyzed the first 27 afterglows detected by *Swift* XRT, and reported that almost all the early X-ray afterglows of *Swift* GRBs do not show a simple power-law flux decline. They show a “canonical” behavior, where the light curve begins with a very steep decay, turns into a very shallow decay  $\sim t^{-0.5}$ , and finally connects to the conventional late-phase afterglow  $\sim t^{-1}$  which is similar to what was observed in the pre-*Swift* era.

---

<sup>1</sup>Department of Physics, Kyoto University, Kyoto 606-8502, Japan; toma@tap.scphys.kyoto-u.ac.jp

<sup>2</sup>Department of Physics, Hiroshima University, Higashi-Hiroshima 739-8526, Japan

The shallow decay phase implies that more time-integrated radiation energy is observed at later time. This is unexpected in the standard model that can explain the late-phase afterglows, i.e., the synchrotron shock model of an impulsive homogeneous jet (Zhang & Mészáros 2004; Piran 2004, for reviews). There seems to be essentially no spectral variation at the transition from the shallow decay phase to the conventional decay phase. This suggests that the origin of the transition is either hydrodynamical or geometrical.

In the hydrodynamical model, the GRB jet is not impulsive but the energy is injected continuously into the blast wave (Zhang et al. 2005; Nousek et al. 2005; Panaiteescu et al. 2005; Granot & Kumar 2005, and references therein). Such a continuous injection can be realized either by the long-lived central engine or the short-lived central engine with some distribution of the Lorentz factors of the launched shells. In the case of the long-lived central engine, the more time-integrated injected energy is required in later time while the injection should be stopped abruptly at some time ( $\sim 10^4$  s). In the case of the short-lived central engine, slower shells should have more energy than faster ones and a lower cut-off of the Lorentz factor should exist. Since the afterglow is dim in the shallow decay phase, the  $\gamma$ -ray efficiency for the front shells is much higher than previously estimated both in the long-lived central engine case and in the short-lived central engine case. This is problematic in the framework of the internal shock model.

In the geometrical model, it is assumed that we observe more energetic regions of the GRB jet later as the afterglow shock decelerates and the visible region increases. The shallow decay phase of the “canonical” afterglow may be a combination of the tail part of the prompt emission and the delayed afterglow emission from an off-axis jet (Eichler & Granot 2005). In this picture, the duration and the flatness of the shallow decay phase correlate with the spectral peak photon energy  $E_p$  and the isotropic  $\gamma$ -ray energy  $E_{\gamma,iso}$ , because all these quantities depend on the viewing angle. The jet break occurs just after the off-axis afterglow is observed, so that the conventional decay phase ( $\sim t^{-1}$ ) is expected to be short. Since Eichler & Granot (2005) discussed a specific “ring-shaped” jet, more general studies for the jet angular structure are desirable to know the general characteristics of geometrical model (see also Panaiteescu et al. 2005).

In this Letter, we develop an inhomogeneous jet model to reproduce the “canonical” X-ray afterglows of GRBs in the framework of the geometrical model. In order to study the angular energy distribution in the jet, we consider an extremely inhomogeneous jet (a multiple-subjet model). Figure 1 illustrates the setup for our analysis of an inhomogeneous jet. We assume that the whole jet (*dashed circle*) consists of multiple subjets (*solid circles*), and the energy injected among subjets is negligible compared to the energy inside each subjet. Each subjet is assumed to make a prompt  $\gamma$ -ray radiation and a subsequent

afterglow following the standard scenario. We calculate the early phase of the afterglow by superposing the contribution of each subjet, and study necessary conditions for reproducing the “canonical” afterglows of the *Swift* GRBs.

The inhomogeneous jet model, such as the multiple-subjet model and the patchy-shell model (Nakamura 2000; Kumar & Piran 2000) has been used to explain the diversity of the prompt emission of GRBs. For example, Toma et al. (2005) discussed the multiple-subjet model to explain the observed  $E_p - E_{iso}$  correlation (see also Yamazaki et al. 2004). The patchy-shell model is also used to explain the observed variability of the early afterglow light curve and the polarization of a particular event like GRB 021004 (e.g., Nakar & Oren 2004).

In § 2, we study the necessary conditions for the jet properties to reproduce the “canonical” afterglows. Summary and discussions are given in § 3.

## 2. Necessary conditions for the shallow decay of early X-ray afterglows

The setup is as follows. We assume that a whole jet consists of multiple subjets. We may consider the initial opening half-angle of each subjet  $\Delta\theta_0^i$  to be  $\gtrsim \Gamma_0^{i-1}$ , where  $\Gamma_0^i \simeq 10^2 - 10^3$  is the initial Lorentz factor of each subjet. The superscript ‘ $i$ ’ and ‘ $w$ ’ denote each subjet and the whole jet, respectively, while the subscript ‘0’ denotes the initial time when each subjet begins to decelerate. Figure 1 shows an example of the initial jet structure. The subjets and whole jet are described by the solid circles and the dashed circle, respectively. Each subjet is assumed to emit the prompt emission by the internal shock and the subsequent afterglow by the synchrotron emission from the external shock of an impulsive homogeneous jet. We assume that all the subjets are ejected at essentially the same time, i.e., over a period that is much shorter than the timescale of the afterglow.

In the following, we discuss the necessary conditions for explaining the “canonical” behavior of X-ray afterglows of *Swift* GRBs. The discussion is separated into two cases: Case (i) the line of sight is along a subjet. Case (ii) the line of sight is off-axis for any subjet. For both cases we will obtain the necessary conditions to reproduce the “canonical” afterglow.

### 2.1. Case (i)

In this case the line of sight is, for example, ‘A’ in Fig 1. The shaded line in Fig 2 shows the afterglow light curve in the range of 2 – 10 keV obtained in our calculation. This demonstrates that in case (i) the “canonical” afterglow light curve can be obtained under

certain conditions explained below.

We calculate X-ray afterglow emission from the external shock of an impulsive homogeneous jet with sharp edge following Panaiteescu & Kumar (2001). The jet dynamics is calculated by the mass and energy conservation equations with the effect of sideways expansion at the local sound speed and radiative energy losses. The initial radius of the shell is set to be 0.01 times the deceleration radius. For the calculation of the synchrotron emission, the spectrum is approximated as a piecewise power law with the injection break  $\nu_m$  and the cooling break  $\nu_c$ . We neglect the self absorption break because we focus on the spectrum for  $\nu > \min(\nu_m, \nu_c)$ . The received flux is calculated by integrating over the equal arrival time surface of photons to the observer. Neither the synchrotron self-Compton emission nor the reverse shock emission is taken into account, for simplicity. In all the following calculations, we fix the initial Lorentz factor of the shell as  $\Gamma_0 = 300$ , the initial opening half-angle of the subjet as  $\Delta\theta_0^i = 0.01$  rad, the number density of the circumburst medium as  $n = 1 \text{ cm}^{-3}$ , the ratio of the magnetic energy and the accelerated electron energy to the shocked thermal energy as  $\epsilon_B = 0.01$  and  $\epsilon_e = 0.1$ , respectively, and the index of the energy distribution function of the accelerated electrons as  $p = 2.3$ .

In Fig 2, the dot-dashed line represents the afterglow light curve expected before the *Swift* era, i.e., the afterglow from a homogeneous jet with a typical afterglow energy of  $E_{k,iso}^w = 10^{52} \text{ erg}$ , an opening half-angle of  $\Delta\theta_0^w = 0.1 \text{ rad}$ , and a viewing angle of  $\theta_v = 0$ . The X-ray afterglow emission has a rising light curve peaking at the shell deceleration time  $t_{\text{dec}} \simeq 5 (E_{k,iso}^w/10^{52} \text{ erg})^{1/3} (\Gamma_0/300)^{-8/3} n^{-1/3} \text{ s}$ . Around this time the XRT band is crossed by  $\nu_m$  and  $\nu_c$  for typical parameters (Sari et al. 1998), so that after the peak, the light curve shows a smooth decline of  $\sim t^{-1.2}$ . The jet break time is estimated as  $t_{\text{jet}}^w \simeq 2 \times 10^4 \text{ s} (\Delta\theta_0^w/0.1 \text{ rad})^{8/3} (E_{k,iso}^w/10^{52} \text{ erg})^{1/3} n^{-1/3} \text{ s}$  (Sari et al. 1999). After this time the light curve steepens into  $\sim t^{-2.3}$ , although the steepening is gradual (see Kumar & Panaiteescu 2000).

The thin solid flat line around  $L_X \sim 10^{50} \text{ erg s}^{-1}$  and for  $t < 10 \text{ s}$  represents a typical prompt burst with a duration of  $\simeq 10 \text{ s}$ . The isotropic X-ray energy is about  $\sim 10^{51} \text{ erg}$ , and for the typical GRB spectrum  $\nu F_\nu \propto \nu$  at low energy, the isotropic  $\gamma$ -ray energy should be about  $\gtrsim 10^{52} \text{ erg}$ . This is comparable to or larger than the afterglow energy  $E_{k,iso}^w = 10^{52} \text{ erg}$  as in the actual observations (Lloyd-Ronning & Zhang 2004). The thin curved solid line for  $t > 10 \text{ s}$  is the tail part of the prompt burst, which comes from the region with large viewing angles in the whole jet. The temporal index of the tail part can be approximated as  $\sim -1 + \beta$ , where  $\beta \sim -2.5$  is the high energy photon index of the prompt emission (e.g., Zhang et al. 2005). Even if the emission regions are so patchy, the tail emission may be smooth since pulses from large viewing angles have long duration and overlap with each

other (Yamazaki et al. 2005).

First, consider the on-axis subjet which includes the line of sight ‘A’ in Fig 1. If the afterglow energy of the on-axis subjet is as large as  $E_{k,iso}^i = 10^{52}$  erg, the afterglow flux is comparable to that of the dot-dashed line. Then it overwhelms the tail part of the prompt emission, and the temporal index of the afterglow emission just after the prompt burst will be  $\sim t^{-1.2}$  or  $\sim t^{-2.3}$ , which is inconsistent with the steep decay observed by XRT. The dashed line (1) in Fig 2 is the afterglow emission from the on-axis subjet with  $E_{k,iso}^i = 3 \times 10^{51}$  erg. Compared to the dot-dashed-line afterglow with  $E_{k,iso}^w = 10^{52}$  erg, we see that the deceleration time  $t_{dec}$  is a little earlier, and the peak luminosity is smaller since the spectral peak flux is  $F_{\nu,\max} \propto E_{k,iso}$ . The jet break time of the subjet is much smaller because of strong dependence of  $t_{jet}^i$  on  $\Delta\theta_0^i$ , and is estimated as  $t_{jet}^i \simeq 30 (\Delta\theta_0^i/0.01 \text{ rad})^{8/3} (E_{k,iso}^i/3 \times 10^{51} \text{ erg})^{1/3} n^{-1/3}$  s. In this case the steep decay due to the tail part of the prompt emission can be observed. Therefore the afterglow energy  $E_{k,iso}^i$  of the on-axis subjet should be at most 1/3 of that of the dot-dashed line which is typical before the *Swift* era.

Secondly, we can show that the shallow afterglow can be produced by the superposition of the subjet emissions. In Fig 2 we show the afterglow emissions from the off-axis subjets, which do not include the line of sight ‘A’. The dashed lines (2), (3), (4), and (5) are the afterglow emissions from the subjets with  $\theta_v^i = 0.025, 0.03, 0.035$ , and  $0.04$  rad, respectively. These subjets are illustrated in Fig 1 and have equal afterglow energies  $E_{k,iso}^i = 3 \times 10^{52}$  erg. This is larger than that of the dot-dashed line by a factor 3. The time at the peak is when the emission from the edge of the subjet arrives at the observer, and is larger for the subjet with larger  $\theta_v^i$  (Granot et al. 2002). The superposed light curve of the on-axis and off-axis subjets is described by the thick solid line, which shows a shallow decline compared to the conventional decline  $\sim t^{-1.2}$ . If all the off-axis subjets have equal viewing angles, the superposition of their contributions produce a bump in our calculation. Nevertheless, the real afterglow may be flat because 2D hydrodynamical simulations show that a rising part of the light curve when viewed with  $\Delta\theta_0^i \lesssim \theta_v^i \lesssim 2\Delta\theta_0^i$  is much flatter than 1D calculations like ours (Granot et al. 2002).

All the subjets expand sideways, and then begin to merge with each other. They will cease to expand sideways because of their pressure, and finally merge into one shell producing the conventional afterglow emission. Although we cannot follow the merging process by our simple calculations, the merged whole jet would make the conventional decline of the dot-dashed line at the late time, since the  $E_{k,iso}^i$  averaged over the solid angle is similar to  $E_{k,iso}^w = 10^{52}$  erg. Therefore we suppose that the shallow decay phase would smoothly connect to the dot-dashed line and the final afterglow would be like the shaded line.

The prompt emission is dominated by that from the on-axis subjet because of the

beaming effect. Thus the prompt burst energy  $E_{\gamma,iso}^i$  of the on-axis subjet is  $\gtrsim 10^{52}$  erg. Since  $E_{k,iso}^i \sim 3 \times 10^{51}$  erg, this implies that the  $\gamma$ -ray efficiency for the on-axis subjet is  $\epsilon_\gamma \equiv E_{\gamma,iso}^i / (E_{\gamma,iso}^i + E_{k,iso}^i) \gtrsim 75\%$ , which is larger than previously estimated. This requirement is similar to the hydrodynamical models for the shallow decay afterglows.

Now what is observed when our line of sight is along the subjet with an energetic afterglow of  $E_{k,iso}^i = 3 \times 10^{52}$  erg? Let us assume that the “canonical” afterglow is observed also in this case. Then the energy of the prompt emission should be  $E_{\gamma,iso} \gtrsim 10^{53}$  erg in order for the tail emission to be larger than the afterglow emission from the on-axis subjet. From the necessary condition for the shallow decay phase obtained in the above discussion, the number of the energetic afterglow subjets should be larger than that of the high  $\gamma$ -ray efficiency subjets. This leads to larger event rate of more energetic prompt bursts, which is not consistent with current observations. Therefore the subjets with energetic afterglows should have low  $\gamma$ -ray efficiency and dim prompt emissions so that they are hard to be observed.

In summary, a subjet making a bright prompt burst should have a dim afterglow and should be surrounded by several subjets with dim prompt bursts and bright afterglows. A favorable GRB jets may have discrete spots with bright bursts and dim afterglows surrounded by the regions with dim bursts and bright afterglows.

## 2.2. Case (ii)

Next, we consider the necessary condition under which the “canonical” afterglow is observed when our line of sight is off-axis for any subjet like ‘B’ in Fig 1. The “canonical” afterglow light curve is obtained by the same calculation as in case (i) removing the contribution from the on-axis subjet. The afterglow light curves from the subjets (2'), (3'), (4'), and (5') in Fig 1 are the same as the dashed lines (2), (3), (4), and (5), respectively. The nearest subjet (2') should have a viewing angle of  $\theta_{v,min} \sim 2\Delta\theta_0^i$ , because if  $\theta_v^i < \theta_{v,min}$  the contribution of the afterglow emission overwhelms the tail part of the prompt emission while if  $\theta_v^i > \theta_{v,min}$  a rising afterglow appears after the tail of the prompt emission. The predicted total afterglow light curve in this case (ii) is similar to that in case (i), i.e., the shaded line.

In case (ii) also, the  $\gamma$ -ray efficiency  $\epsilon_\gamma$  should be large. The prompt emission is dominated by the subjets with the viewing angles  $\theta_v^i \sim \theta_{v,min}$ . If the velocity of a point source has an angle  $\theta$  with the line of sight, the observed energy from this source is  $\propto (1 - \beta \cos \theta)^{-3}$  because of the beaming effect. The observed energy from widely distributed segments of size  $\Delta\theta_0^i$  with similar viewing angles  $\theta_{v,min}$  roughly follows  $E_{\gamma,iso} \propto [1 - \beta_0^i \cos(\theta_{v,min} - \Delta\theta_0^i)]^{-2}$

(Toma et al. 2005; Eichler & Levinson 2004). This is derived by the integration of the contribution of the point source over solid angle occupied by the emission regions. Thus, in this case with  $\theta_{v,\min} \sim 2\Delta\theta_0^i$ , we receive the prompt burst energy  $E_{\gamma,iso} \sim (1 - \beta_0^i \cos \Delta\theta_0^i)^{-2} E_{\gamma,iso}^i \simeq (\Gamma_0^i \Delta\theta_0^i)^{-4} E_{\gamma,iso}^i$ , where  $E_{\gamma,iso}^i$  is the isotropic energy of the prompt emission when a subjet is viewed on-axis. The received prompt energy is  $E_{\gamma,iso} \gtrsim 10^{52}$  erg in the above calculation, and thus  $E_{\gamma,iso}^i \gtrsim 10^{54}$  erg. Since  $E_{\gamma,iso}^i = 3.0 \times 10^{52}$  erg, we obtain  $\epsilon_\gamma \gtrsim 97\%$ . If this case occurs dominantly over the case (i), we should observe many very bright GRBs, when the line of sight is along the  $\gamma$ -ray bright subjet. Thus the contribution of this case to the shallow decay afterglows would be small.

### 3. Discussion

We have investigated early X-ray afterglows of GRBs within inhomogeneous jet models by using a multiple-subjet model. We find that several off-axis subjets can reproduce the shallow decay phase of the light curves observed by *Swift* XRT. The shallow decay phase is produced by the superposition of the afterglows from off-axis subjets, and it connects to the conventional late-phase afterglow which is produced by the merged whole jet. The flux decay index during the shallow phase is determined by the configuration and afterglow energies of subjets.

We found necessary conditions for obtaining the “canonical” afterglow by separating our discussions into two cases, i.e., whether the line of sight is along a subjet (case (i)) or not (case (ii)). In both cases (i) and (ii), subjets producing a bright prompt emission should have  $\gamma$ -ray efficiency larger than previously estimated. This requirement is similar to the hydrodynamical model (Zhang et al. 2005; Nousek et al. 2005) and is problematic in the framework of the internal shock model.

There are some caveats and predictions in our model. First, in case (i), a subjet producing a bright prompt burst should have a dim afterglow emission and should be surrounded by several subjets producing a dim prompt and a bright afterglow emissions. When the line of sight is along the subjet with a dim prompt and a bright afterglow emissions, the conventional afterglow light curve without a shallow phase is observed. Therefore we predict that small  $E_{\gamma,iso}$  events should have the conventional afterglow light curve. Among 10 *Swift* GRBs with known redshifts, GRB 050416A has an extremely small  $E_{\gamma,iso}$  of  $\lesssim 10^{51}$  erg and does not have a shallow decay phase (Nousek et al. 2005). This event may support the case (i) of the inhomogeneous jet model, although more statistics is required to confirm the validity. Secondly, the number of subjets with dim bursts and bright afterglows should be several times larger than that of the observed  $\gamma$ -ray bright subjet. Then the true GRB rate

should be several times larger than the current estimates. In addition, since many subjets are  $\gamma$ -ray dark, the mean  $\gamma$ -ray efficiency over the whole jet does not need to be so large (Kumar & Piran 2000). Only a subjet that happens to emit almost all energy into  $\gamma$ -ray may be observed as a GRB.

Case (ii) suggests that for most events both the prompt and the afterglow emissions arise from off-axis viewing angles, which is similar to the scenario of Eichler & Granot (2005). In this case, we found that most of the subjets should produce a bright prompt and a dim afterglow emissions. When the line of sight is along such a subjet, the conventional but dim afterglow is observed. Then we predict that there should be large  $E_{\gamma,iso}$  events with a conventional afterglow in case (ii). We should observe such bright  $\gamma$ -ray events with a similar order of rate as the “canonical” events, which may be tested in future.

We thank G. Sato and T. Takahashi for useful discussions. This work is supported in part by Grant-in-Aid for the 21st Century COE “Center for Diversity and Universality in Physics” from the Ministry of Education, Culture, Sports, Science and Technology (MEXT) of Japan and also by Grants-in-Aid for Scientific Research of the Japanese Ministry of Education, Culture, Sports, Science, and Technology 14047212 (K. I. and T. N.), 14204024 (K. I. and T. N.) and 17340075 (T. N.).

## REFERENCES

Chincarini, G., et al. 2005, preprint (astro-ph/0506453)  
Cusumano, G., et al. 2005, preprint (astro-ph/0509689)  
Eichler, D., & Granot, J. 2005, preprint (astro-ph/0509857)  
Eichler, D., & Levinson, A. 2004, ApJ, 614, L13  
Granot, J., Panaiteescu, A., Kumar, P., & Woosley, S. 2002, ApJ, 570, L61  
Granot, J., & Kumar, P. 2005, preprint (astro-ph/0511049)  
Hill, J. E., et al. 2005, preprint (astro-ph/0510008)  
Kumar, P., & Panaiteescu, A. 2000, ApJ, 541, L9  
Kumar, P., & Piran, T. 2000, ApJ, 535, 152  
Lloyd-Ronning, N. M. & Zhang, B. 2004, ApJ, 613, 477

Nakamura, T. 2000, *ApJ*, 534, L159

Nakar, E., & Oren, Y. 2004, *ApJ*, 602, L97

Nousek, J. A., et al. 2005, preprint (astro-ph/0508332)

Panaitescu, A., & Kumar, P. 2001, *ApJ*, 554, 667

Panaitescu, A., Mészáros, P., Gehrels, N., Burrows, D., & Nousek, J. A. 2005, preprint (astro-ph/0508340)

Piran, T. 2004, *Rev. Mod. Phys.*, 76, 1143

Sari, R., Piran, T., & Narayan, R. 1998, *ApJ*, 497, L17

Sari, R., Piran, T., & Halpern, J. 1999, *ApJ*, 519, L17

Tagliaferri, G., et al. 2005, *Nature*, 436, 985

Toma, K., Yamazaki, R., & Nakamura, T. 2005, *ApJ* in press, preprint (astro-ph/0504624)

Vaughan, S., et al. 2005, preprint (astro-ph/0510677)

Yamazaki, R., Toma, K., Ioka, K., & Nakamura, T. 2005, preprint (astro-ph/0509159)

Yamazaki, R., Ioka, K., & Nakamura, T. 2004, *ApJ*, 606, L33

Zhang, B., Fan, Y. Z., Dyks, J., Kobayashi, S., Mészáros, P., Burrows, D. N., Nousek, J. A., & Gehrels, N. 2005, preprint (astro-ph/0508321)

Zhang, B., & Mészáros, P. 2004, *IJMPA*, 19, 2385

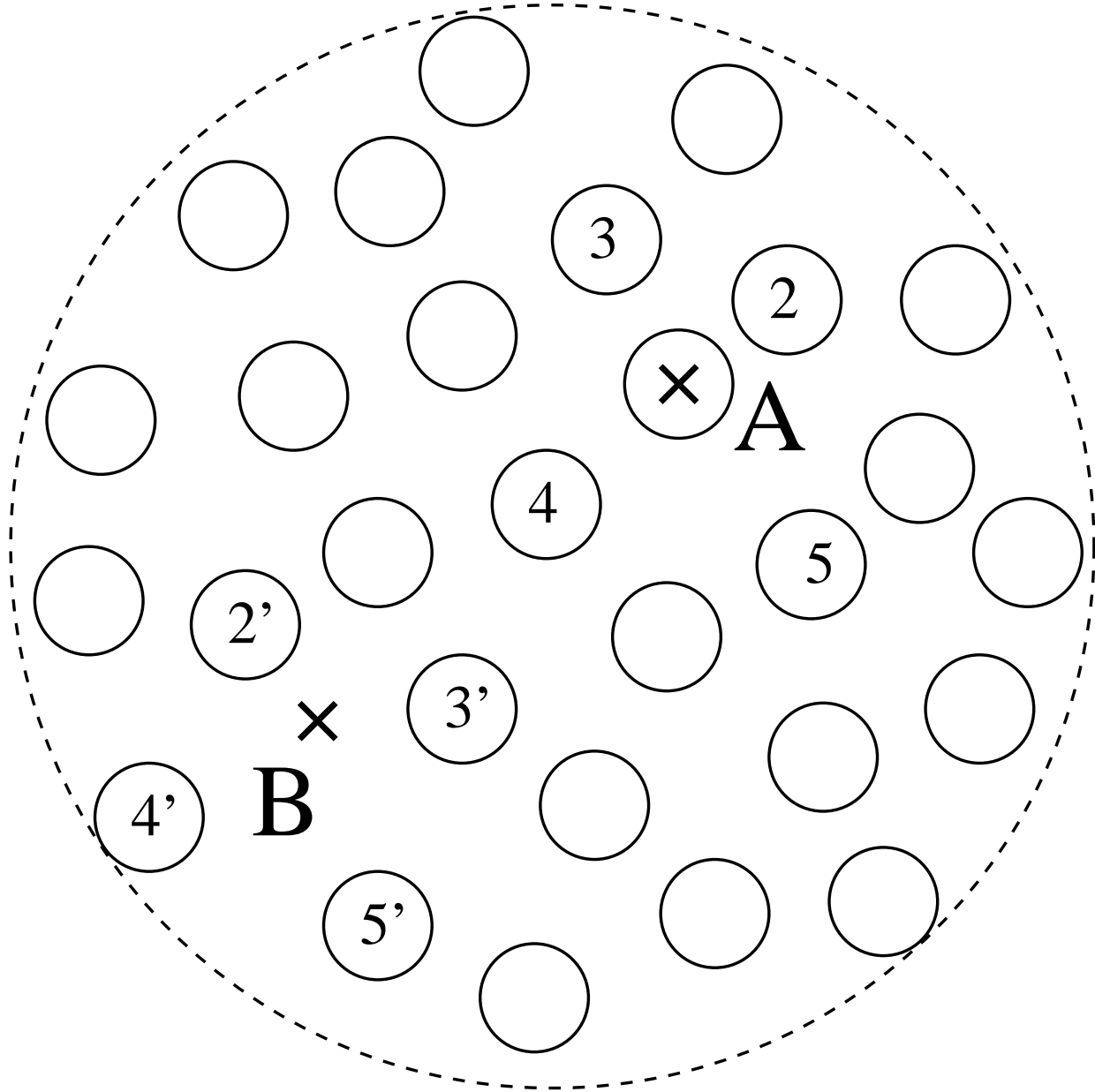


Fig. 1.— Setup for our analysis of an inhomogeneous jet. A whole jet (*dashed circle*) consists of multiple subjets (*solid circles*). Points ‘A’ and ‘B’ describe the lines of sight for our calculations in § 2.1 and § 2.2, respectively. For our calculations of the early afterglows from the inhomogeneous jet we take the initial opening half-angle of the subjets and the whole jet as  $\Delta\theta_0^i = 0.01$  rad and  $\Delta\theta_0^w = 0.1$  rad. Subjets (2), (3), (4), and (5) for the line of sight ‘A’ (similarly, (2'), (3'), (4'), and (5') for the line of sight ‘B’) have the viewing angles  $\theta_v^i = 0.025, 0.03, 0.035$ , and  $0.04$  rad.

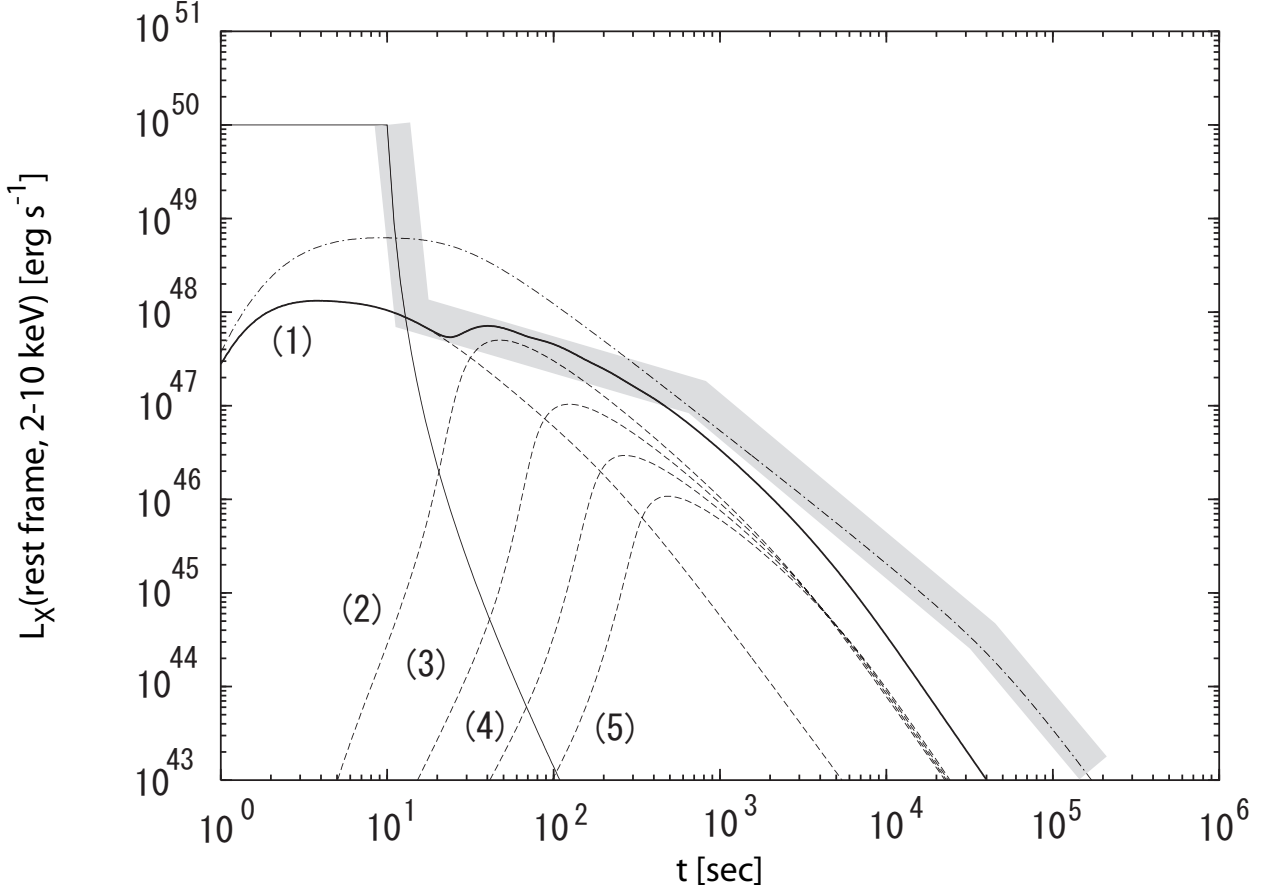


Fig. 2.— Example of the afterglow light curve (the isotropic-equivalent luminosity) in the range 2–10 keV measured in the cosmological rest frame of the GRB. The dot-dashed line is the afterglow from a jet with  $E_{k,iso}^w = 10^{52}$  erg,  $\Delta\theta_0^w = 0.1$  rad, and  $\theta_v = 0$ . The thin solid flat line for  $t < 10$  s represents a typical prompt burst which corresponds to the late-phase of the dot-dashed-line afterglow. The thin solid curved line  $t > 10$  s represents the tail part of the prompt emission which we set as  $\propto (t - 9.0)^{-3.5}$ . The dashed line (1) is the afterglow from a subjet with  $E_{k,iso}^i = 3 \times 10^{51}$  erg,  $\Delta\theta_0^i = 0.01$  rad, and  $\theta_v^i = 0$ . The dashed lines (2), (3), (4), and (5) are the afterglows from subjets with  $E_{k,iso}^i = 3 \times 10^{52}$  erg,  $\Delta\theta_0^i = 0.01$  rad, and  $\theta_v^i = 0.025, 0.03, 0.035$ , and  $0.045$  rad, respectively. These subjets correspond to (2), (3), (4), and (5) for the line of sight ‘A’ (or (2'), (3'), (4'), and (5') for the line of sight ‘B’) in Fig 1. The thick solid line is the superposition of all the dashed lines (1)–(5). The shaded line is what we expect for the afterglows from inhomogeneous GRB jets.